ANALYSIS OF BEAMFORMING FROM VARIOUS TRANSDUCER SHAPE

LUMINITA MORARU[1], LAURA ONOSE[2]

[1] *"Dunarea de Jos" University of Galati, Faculty of Sciences, 800201, Galati, Romania*

[2] *Metallurgic Industrial Scholar Group, 800511, Galati, Romania*

Abstract. *Medical ultrasound data suffers from blur caused by the volume expansion of the pressure field of the mechanical wave. This blur is dependent on the used excitation signal and focusing of the ultrasonic wave and can therefore be examined and manipulated to compute a set of better parameters for deconvolution on the data in order to improve overall system resolution. Looking at the ultrasound transfer function we can focus on the examination of the "point spread function" and ways to influence its size especially in the lateral direction. A method of simulating sound pressure with the aid of the impulse response is applied to a various shaped ultrasonic radiators. We focus our attention on the peak appearance in the pressure response of the transducers.*

Keywords: *beamforming, transducer, ultrasound.*

1. INTRODUCTION

In the late 60's, early 70's, Tupholme and Stepanishen [1, 2] introduced the impulse response method theory to model acoustic fields. This method is based on linear acoustics and can be used to model acoustic fields and responses for both single transducer setups and for array imaging. The imaging system is divided in two parts: the first one accounts for acoustical wave propagation effects from the transducer surface to the observation point, and the second one accounts for the electro-acoustical effects. By convolved these two parts are then obtained a model for the total imaging system.

The impulse response method is based on the assumption that the transducer can be treated as a baffled piston. This assumption implies that is only need to consider the active area of the transducer when modeling the wave propagation. The pressure at an observation point *r* is described by the Rayleigh integral formula which simply states that the acoustic field at an observation point is the sum of the contributions from all points of the active area of the transducer.

$$p(r,t) = \rho_0 \frac{\partial}{\partial t} v_n(t) * h(r, t - t_0) \tag{1}$$

where $v_n(t)$ is normal velocity, uniform on the transducer's surface, $h(r,t)$ is *spatial impulse response* (SIR). Since the normal velocity depends on both the input signal, *u(t)*, and the electro-acoustical properties of the transducer, it can be described with the electrical impulse response $h^{ef}(t)$.

The pressure at *r* can be expressed by the convolutions of the input signal and the two impulse responses

$$p(r,t) = h(r,t) * h^{ef}(r,t) * u(t) \tag{2}$$

Double-path (pulse-echo) responses can be treated in a similar way by convolving the forward response with the backward electrical (acoustic-electrical) response and the backward SIR for a point source at *r*.

For a circular disc (Fig. 1) the spatial impulse response supports an analytical solution [3] which can be obtained for both two situations: when the observation point is inside the aperture of the disc and when is outside the aperture. The disc is assumed to be located in the *xy* plane centered at $x = y = 0$ and the distance in the *xy* plane from the center axis of the disc to the observation point is given by $r = \sqrt{x^2 + y^2}$. The earliest time that the wave reaches the observation point *r* is $t_z = \frac{z}{v}$. the propagation time corresponding to the edges of the disc that are closest from *r* is $t_r = \frac{r}{v}$ and the propagation times corresponding to the edges of the disc that are furthermost away from *r* is $t_{1,2} = t_z\sqrt{1+\left(\frac{a \mp r}{z}\right)^2}$.

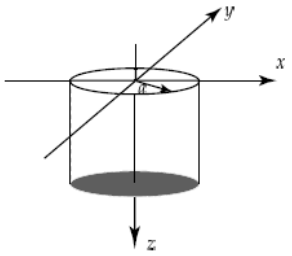

Fig. 1. Geometry of a circular disc source.

For the first case, when the observation point is inside the aperture of the disc, $r \le a$, the circular disc spatial impulse response is given by:

$$h(r,t) = \begin{cases} 0, & t \le t_z \\ v, & t_z \le t \le t_1 \\ \frac{v}{\pi}\cos^{-1}\left(v^2\frac{t^2 - t_z^2 + t_r^2 - a/v^2}{2t_r\sqrt{t^2 - t_z^2}}\right) & t_1 < t \le t_2 \\ 0, & t > t_2 \end{cases} \tag{3}$$

For the second case, when the observation point is outside the aperture of the disc, $r > a$, the circular disc spatial impulse response is given by:

$$h(r,t) = \begin{cases} 0, & t \le t_1 \\ \frac{v}{\pi}\cos^{-1}\left(v^2\frac{t^2 - t_z^2 + t_r^2 - a/v^2}{2t_r\sqrt{t^2 - t_z^2}}\right) & t_1 < t \le t_2 \\ 0, & t > t_2 \end{cases} \tag{4}$$

Since the on-axis SIR has duration $t_1 - t_z$ with the constant amplitude *v* in the time interval $t_z \le t \le t_1$, the pulse amplitude is constant regardless of the distance to the observation point. At $z = 0$ the duration is $t_1 = a/v$. As the distance increases the duration of the SIR

becomes shorter, and for large z it approaches to the delta function. The transducer size effects are therefore most pronounced in the near-field.

For many transducer geometries there exist no analytical solutions. Hence this situation supports numerical methods, and was developed programs which permits simulation and modeling complex transducer shape. One of this is The DREAM Toolbox [4] which can simulate ultrasonic measurement systems for many configurations including phased arrays and measurements performed in loss media.

2. SIMULATION RESULTS AND DISCUSSION

For two different value of sound speed (for tissue is 1450 m/s respectively 330 m/s in air) and for three different distance z: z_1=5 mm, z_2=10 mm, z_3=20 mm it was calculated the pressure response from a single transducer. In this study were considered three types of transducer geometry: circular disc with *r=10 mm* (Fig. 1), spherical concave with *r =10 mm R=100 mm* (Fig. 2) and cylindrical concave with *a=10 mm, b=20 mm* and *R=100 mm* (Fig. 3).

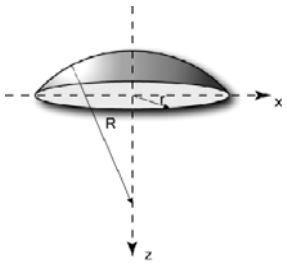

Fig. 2. Geometry of a spherical concave source.

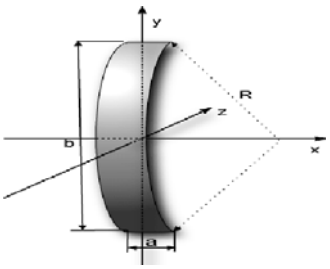

Fig. 3. Geometry of a cylindrical concave source.

In Figs. 4 and 5 are presented the pressure response for a circular disc. This situation corresponds to analytical solution: a main lobe with many side lobes.

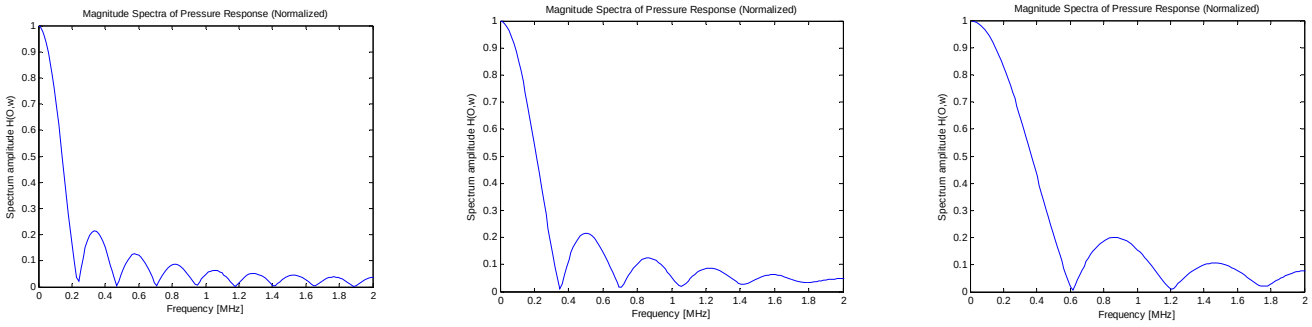

(a) **(b)** **(c)**

Fig. 4. The pressure response at z_1=5mm(a), z_2=10 mm(b), z_3=20mm(c) from a circular disc (1450m/s).

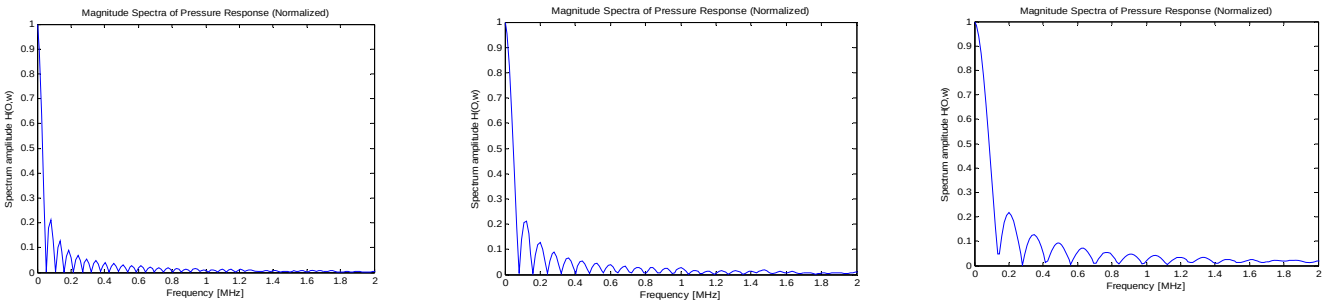

(a) (b) (c)

Fig. 5. The pressure response at z_1=5mm(a), z_2=10 mm(b), z_3=20mm(c) from a circular disc (330m/s).

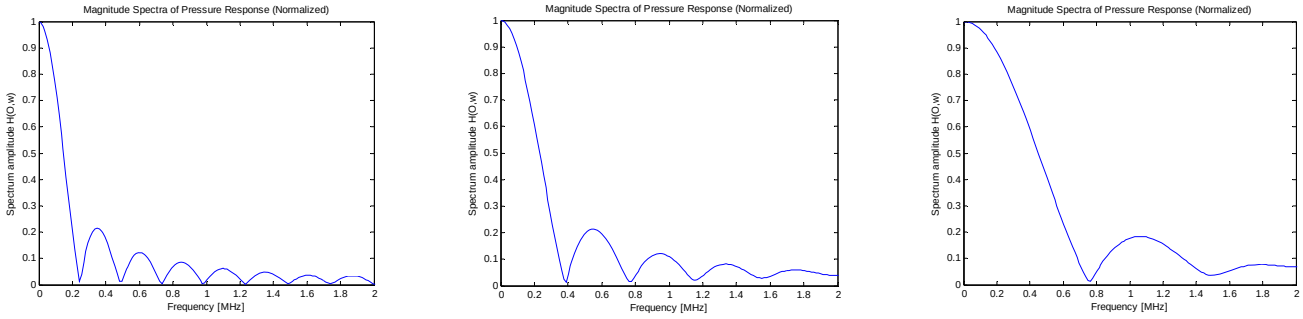

(a) (b) (c)

Fig. 6. The pressure response at z_1=5mm(a), z_2=10 mm(b), z_3=20mm(c) from a spherical concave source (1450m/s).

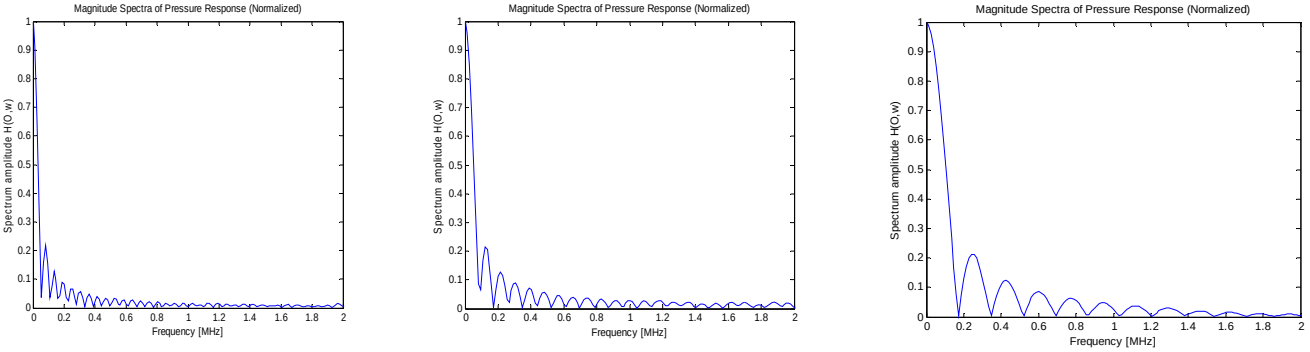

(a) (b) (c)

Fig. 7. The pressure response at z_1=5mm(a), z_2=10 mm(b), z_3=20mm(c) from a spherical concave source (330m/s).

For more complex geometry such is cylindrical concave source, the pressure response spectra presented in Figs. 8 and 9 is different.

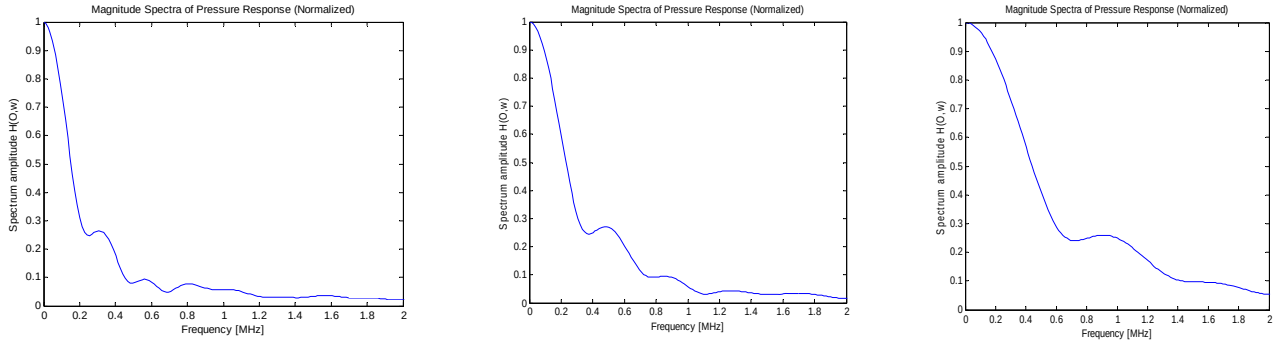

(a) **(b)** **(c)**

Fig. 8. The pressure response at z_1=5mm(a), z_2=10 mm(b), z_3=20mm(c) from a cylindrical concave source (1450m/s).

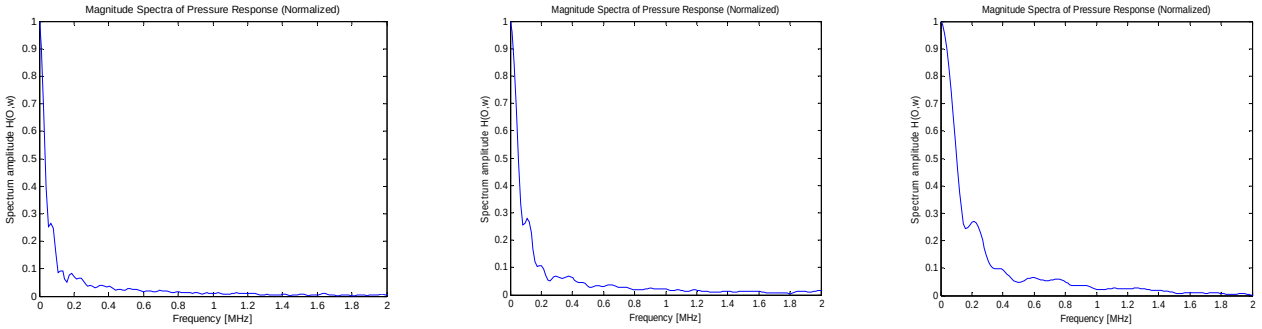

(a) **(b)** **(c)**

Fig. 9. The pressure response at z_1=5mm(a), z_2=10 mm(b), z_3=20mm(c) from a cylindrical concave source (330m/s).

Figs. 8 and 9 shows the frequency response calculated at various distances from the front of the transducer. It is noteworthy that the existence and the number of dominant peaks are different to the measured data in Figs. 4-7. The side lobes are lower and indicate that energy is concentrated in the main lobe.

3. CONCLUSIONS

Using simulation tools, we investigated a method for analyzing the pressure response of ultrasonic transducers. Optimum geometry of transducers to improve performance is analyzed. As important remark we highlight: at an ultrasonic speed, one dominant peak (main lobe) was seen in the sound pressure response of the transducer, and many secondary peaks (side lobes) were seen in the transducer with simple geometry. For complex geometry (*i.e.* cylindrical concave source) we obtain a better pressure response of the transducers.

REFERENCES

[1] Piwakowski, B., Sbai, K., *IEEE Transactions on Ultrasonics, Ferroelectrics and Frequency Control,* **46**, 422–440, 1999.
[2] Tupholme, G. E., *Mathematika* **16**, 209–224, 1969.
[3] Stepanishen, P., *J. Acoust. Soc. America,* **49**, 1629–1638, 1971.

[4] Lingvall, F., *User Manual for the DREAM Toolbox Version 2.1.3 an ultrasound simulation software for use with Matlab and GNU Octave*, 2009.
[5] Onose, L., Moraru, L., *Annals of the "Dunarea de Jos" University of Galaţi, Mathematics, Physics, Chemistry, Informatics*, II (XXXII), Fascicle II, supplement, 49–53, 2009.
[6] Onose, L., Moraru, L., Onose, D., *Annals of the "Dunarea de Jos" University of Galaţi, Mathematics, Physics, Chemistry, Informatics*, II (XXXII), Fascicle II, supplement, 65–69, 2009.

Manuscript received: 30.04.2010
Accepted paper: 19.07.2010
Published online: 04.10.2010